A hydrogen-permselective amorphous silica membrane derived from polysilazane

Y. Iwamoto*, K. Sato, T. Kato, T. Inada, Y. Kubo

Japan Fine Ceramics Center, 2-4-1, Mutsno, Atusta-ku, Nagoya 456-8586, Japan

Abstract

A microporous amorphous silica membrane has been synthesized by thermal conversion in air of polysilazane on a silicon nitride (Si_3N_4) porous substrate. The porous substrate near the surface layer was penetrated by polysilazane, and converted into mesoporous amorphous silica/Si_3N_4 composite layer. Then, an active molecular sieving microporous amorphous silica thin layer was synthesized on the surface of the mesoporous composite layer. The polysilazane-derived amorphous silica membrane exhibited H_2 permeance of 1.3×10^{-8} mol/m^2 s Pa at 573 K, and the permeability ratio of H_2/N_2 was measured to be 141. The effects of heat treatment condition on the meso/microporous structure development of the polysilazane-derived amorphous silica within the Si_3N_4 porous substrate are discussed from a viewpoint of fabricating hydrogen-permselective amorphous silica membranes through polymeric precursor route.
© 2004 Elsevier Ltd. All rights reserved.

Keywords: Polysilazane; Polymeric; Amorphous silica; Membrane

1. Introduction

Ceramic membranes with micropores smaller than 1 nm have great potential for gas separation. Compared to polymer membranes, microporous ceramic membranes with molecular sieve-like properties have relatively high gas permeances and a good stability at higher temperatures. Moreover, microporous ceramic membranes can be expected to use in membrane reactors for conversion enhancement in dehydrogenation[1] and methane reforming reactions[2–5] for hydrogen production.

Hydrogen-permselective amorphous silica-based membranes have been synthesized using chemical vapor deposition (CVD)[4,6–10] and sol–gel technique.[5,11–16] Amorphous silicon oxycarbide (Si–C–O) membranes have been synthesized from polycarbosilane[17,18] or polydimethylsilane.[19] In this polymer pyrolysis route, oxygen was partially introduced to the polymeric precursor-derived Si–C film in air, and subsequent pyrolysis under inert atmosphere yielded Si–C–O membranes with H_2/N_2 permselectivity.

Generally, a microporous ceramic membrane can be fabricated on a porous support, and an important structural feature is a mesoporous intermediate layer, i.e., γ-alumina (Al_2O_3), which is placed in between the layer of a hydrogen-permselective microporous thin layer on the upper side and the surface of an α-Al_2O_3 porous support on the inner side.[5,12–14,16,18] The mean pore size of the mesoporous γ-Al_2O_3 intermediate layer is controlled to be about 4 nm. However, a small amount of larger macropores sometimes exists in the intermediate layer, which leads to the formation of pinholes or cracks in the microporous ceramic membranes. To develop high-performance hydrogen separation membranes, it is important to develop technologies for fabricating a fine mesoporous intermediate layer as well as fabricating a molecular-sieve microporous membrane.

Recently, an interesting method for fabrication of amorphous silica thick coatings has been reported.[20] Perhydropolysilazane (PHPS), a polymeric precursor for Si_3N_4 ceramics can be coated on various types of substrates. The PHPS-derived Si–N precursor film is easily oxidized and converted into an amorphous silica thick coating by pyroylsis in air. During this thermal conversion process, nitrogen and hydrogen of the PHPS are fully substituted with oxygen, which leading to the formation of the clack-free thick and

* Corresponding author. Tel.: +81 52 871 3500; fax: +81 52 871 3599.
E-mail address: iwamoto@jfcc.or.jp (Y. Iwamoto).

highly dense amorphous silica coating. If the porosity of the polymeric precursor-derived amorphous silica coating can be controlled in the micro/mesopore size range, this synthesis route can be expected to apply for fabricating an amorphous silica mesoporous intermediate layer as well as for a molecular sieve microporous amorphous silica membrane.

In this study, a commercial organo-substituted polysilazane is selected as a starting polymeric precursor to control the porosity of the resulting amorphous silica. Then, an amorphous silica membrane is synthesized by thermal conversion in air of the polysilazane on a Si_3N_4 porous substrate. The porous substrate near the surface layer can be penetrated by the polysilazane, and converted into amorphous silica/Si_3N_4 composite layer. The pore-size distribution of the polysilazane-derived amorphous silica in the composite layer is controlled so as to make the composite layer as a fine mesoporous intermediate layer. An active molecular sieving amorphous silica thin layer is synthesized on the surface of the mesoporous intermediate layer. The membrane exhibits hydrogen permselectivity, comparable with other amorphous silica or silicon oxycarbide membranes in literature.

2. Experimental procedure

2.1. Preparation of Si_3N_4 porous substrates

Si_3N_4 porous substrates were prepared in our laboratory. Commercial α-Si_3N_4 (Grade SN-E10, $d_{50} = 0.45\,\mu m$, Ube Co., Yamaguchi, Japan) was doped with sintering aids of 5 wt.% α-Al_2O_3 (Grade AKP-30, $d_{50} = 0.34\,\mu m$, Sumitomo Chemical Co., Tokyo, Japan) and 5 wt.% Y_2O_3 (Grade NRN, $d_{50} = 0.28\,\mu m$, Daiichi Kigenso Kagaku Kogyo Co., Osaka, Japan). The doped powder was mixed with 22.2 vol.% of carbon powder (Turbostratic graphite, Grade MA77, $d_{50} = 0.023\,\mu m$, Mitsubishi Chemical Co., Tokyo, Japan) by ball-milling for 96 h using EtOH, then dried and sieved by 250 μm screen mesh. The sieved powder was uniaxially pressed at 5 MPa into a disc with a diameter of 20 mm. The green compact was placed in a BN coated graphite die and hot pressed at 1823 K for 2 h at a stress of 40 MPa under N_2 atmosphere (98 kPa). The hot pressing was carried out in a graphite resistance-heated furnace (Model High Multi 10000, Fujidempa Kogyo, Osaka, Japan). The hot pressed specimen was machined into a disc of 10 mm (W) $\times$ 10 mm (L) $\times$ 1.0 mm (T). Then, the residual carbon in the specimen was burned out by heat treatment at 873 K in air for 24 h. The Si_3N_4 porous substrate was characterized using mercury porosimetry (Model Autopore III, Micromeritics Instrument Co., Norcross, GA). Typical pore-size distribution of the porous substrate is shown in Fig. 1. The mean pore size and porosity were measured to be 80 nm and 28%, respectively.
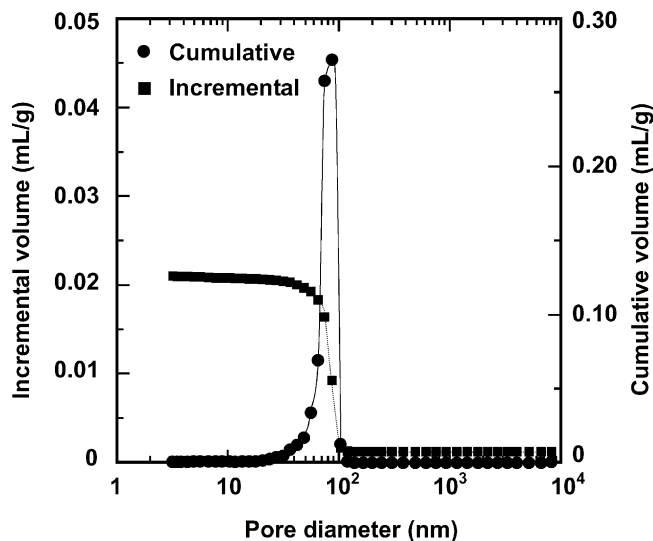

Fig. 1. Pore-size distribution of a Si_3N_4 porous substrate.

2.2. Evaluation of PSZ-derived amorphous silica

Polysilazane (PSZ, Tonen Co., N-N 710, average molecular weight of 1500, empirical formula: $SiN_{0.79}C_{0.62}H_{2.21}$, Tokyo, Japan) was used as-received. The structural units of the PSZ identified by ^{1}H and ^{29}Si NMR spectroscopy were SiH_xN_{4-x} ($x = 1$–3) and $Si(CH_3)HN_2$.[21]

The Si_3N_4 porous substrate was immersed in a 20 wt.% xylene solution of PSZ, and placed in a 10 ml flask. The flask was evacuated so that the porous substrate was penetrated by PSZ. The sample substrate was placed in a furnace, and heat-treated at 543 K for 1 h under N_2 atmosphere (cross-linked in N_2), or cured at 543 K for 1 h in air. Finally, the sample substrate was heat-treated at 873 K in air for 10 h. The thermal behavior of PSZ during the heat treatment mentioned above, was studied by thermogravimetric (TG) analysis (Model TG8110D, Rigaku, Tokyo, Japan) and Fourier Transform infrared (FT-IR) spectroscopic analysis (Model System 2000, Perkin-Elmer, Boston, MA). The sample used for these analyses was prepared by collecting powdered residue after drying the precursor solution at 323 K. The FT-IR spectra were recorded on KBr pellets containing precursor samples. The pore volume and pore-size distribution of the PSZ-derived amorphous silica within a Si_3N_4 porous substrate were evaluated by N_2 sorption isotherm analysis (Model Autosorb-1, Quantachrome Instruments, Boynton Beach, FL). The micropores ($r_{pore} < 2.0\,nm$) and mesopores ($2.0\,nm \leqq r_{pore} < 50\,nm$) of the PSZ-derived amorphous silica were characterized by the SF[22] and BJH[23] method, respectively.

2.3. Synthesis and characterization of amorphous silica membranes

The 20 wt.% PSZ solution was spin-coated and penetrated into near the surface layer of the Si_3N_4 porous substrate.
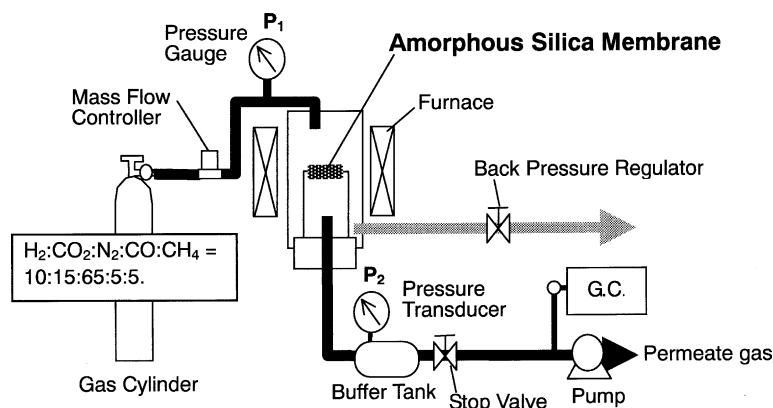
Fig. 2. Schematic of apparatus for gas permeation measurements.

The PSZ was cross-linked at 543 K in N_2 for 1 h with a heating and cooling rate of 2 K/min. The procedure of spin-coating and cross-linking was repeated three times. Then, the surface layer was converted into mesoporous amorphous silica/Si_3N_4 composite layer by heat treatment at 873 K in air for 10 h with a heating and cooling rate of 2 K/min. To fabricate an active molecular sieving thin layer, a PSZ precursor film was prepared on the surface of the mesoporous composite layer using a spin-coating technique. The precursor film was cured at 543 K for 1 h followed by an additional heat treatment at 873 K in air for 10 h with a heating and cooling rate of 2 K/min. The process of spin-coating, curing and heat treatment was repeated twice.

Permeances through the amorphous silica membrane were determined using a mixed gas of H_2, CO_2, N_2, CO and CH_4 in the ratio 10:15:65:5:5. Each gas was of high purity, >99.99%. The gas permeance measurements were performed at temperatures ranging from 423 to 573 K. The setup for the measurements is illustrated in Fig. 2. The disc-type membrane was fixed on a quartz tube in a stainless steel cell. The permeate side was evacuated by rotary pump, then the mixed gas was introduced into the cell, and the feed side (P_1) and the permeate side (P_2) were maintained at 101.3 and 4.0 kPa, respectively. The stop valve on the permeate side was closed, and the time (Δt) taken for the permeate side pressure to reach 6.6 kPa was recorded. The permeating flux (F) was calculated using Eq. (1)

$$F \ [\text{mol/m}^2 \ \text{s}] = \frac{V/SRT}{\Delta t/\Delta P_2} \tag{1}$$

where V is the total volume of the buffer tank and gas line [m^3], S is the membrane area [m^2], R is the gas constant [J/K mol], T is the temperature [K], and ΔP_2 has a constant value of 2.2 kPa.

The permeate gas composition was analyzed using a gas chromatograph (GC, Model MicroGC 2002, CHROMPACK Co., Middelburg, the Netherlands), and the permeance (P_i)

of gas i was calculated using Eq. (2)

$$P_i \ [\text{mol/m}^2 \ \text{s Pa}] = \frac{FM_i^p}{P_1 M_i^f - P_2 M_i^p} \tag{2}$$

where P_i is the feed gas pressure of 101.3 kPa, P_2 is the logarithmical average of 4.0 and 6.6 kPa, i.e., 5.2 kPa, M_i^f and M_i^p are molar fractions of gas i on the feed side and permeate side, respectively.

Permselectivity is defined as the permeance ratio of two gases. For example, the H_2/N_2 permselectivity is given by the ratio P_{H_2}/P_{N_2}.

Microstructure of the amorphous silica membrane on the Si_3N_4 porous substrate was studied using a transmission electron microscopy (TEM, Model EM-002B, Topcon Co., Tokyo, Japan, operating at 200 kV). The TEM sample specimen was prepared using a focused ion beam (FIB) equipment (Model FB-2100, Hitachi Co., Tokyo, Japan).[24]

3. Results and discussion

3.1. Thermal analysis and porous structure development

TG curve in N_2 of PSZ is shown in Fig. 3a. The TG curve indicates two apparent weight losses located between 340 and 504 K, and 543 and 782 K. The total weight loss at 1273 K is measured to be 22%. The first weight loss of 5.7% is caused by the evaporation of residual xylene.[25,26] The second weight loss of 14% is due to mainly the evolution of lower molecular weight silazane compounds.[27] During heat treatment up to 1273 K, several exothermic peaks are observed at 543 to 973 K, which indicating that the cross-linking reactions to form Si−N−Si linkages take place in this temperature range.[28,29]

The TG curve in air of PSZ is shown in Fig. 3b. The weight loss up to 543 K is 0.5%, which is much suppressed in comparison with that in N_2. Then, the TG curve exhibits two weight gains located at 543 to 773 K and at 773 to 898 K. Finally at 1273 K, the total weight gain reaches 13%. During
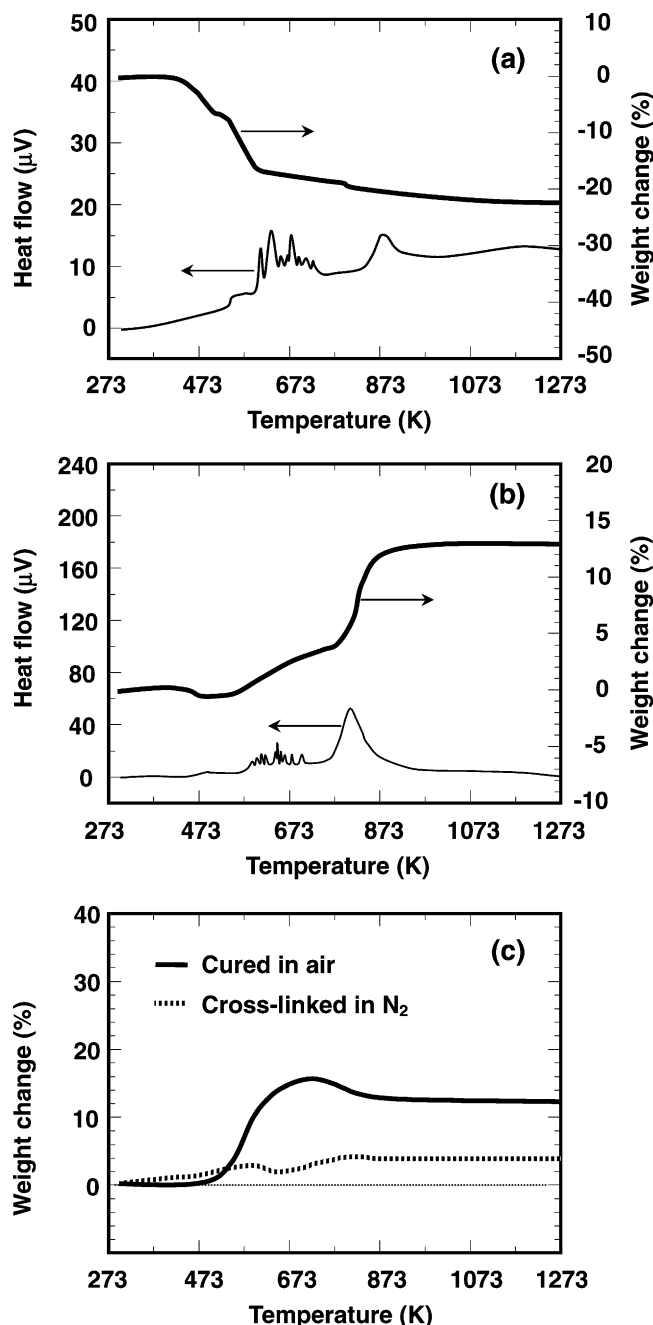
Fig. 3. Thermal behavior of PSZ in (a) N$_2$ and (b) air. (c) TG curves of cross-linked and cured PSZ.

the first weight gain of 4.5%, several small exothermic peaks are observed, while the second weight gain of 9% is accompanied by an apparent one exothermic peak. These results reveal that the oxidation of PSZ has already started at 543 K, and the oxidation of Si–H bonds is thought to be the main reaction up to 543 K.[30]

$$2 \equiv Si\text{–}H + O_2 \rightarrow \equiv Si\text{–}O\text{–}Si \equiv + H_2O \qquad (3)$$

The actual detailed mechanism might involve the formation of free radicals as previously suggested for the oxygen-curing of polycarbosilane[31] or polycarbosilazane,[30] and the forma-

tion of stable Si–O–Si linkages suppressed the evolution of the light weight molecules. During the two weight gains observed at 543 to 898 K, the nitrogen and hydrogen in the PSZ could be fully substituted by oxygen.

The evaporation of the lightweight molecules in the PSZ was found to depend on the atmosphere of heat treatment, which was expected to change the porous structure of the PSZ-derived amorphous silica. Therefore, the temperature for cross-linking in N$_2$ or curing in air was selected to be 543 K, and further thermal behaviors in air of the cross-linked PSZ and cured PSZ were studied. As shown in Fig. 3c, the TG curve of the cured PSZ exhibits a remarkable weight gain at 504 to 704 K. Then, weight loss occurs at 704 to 873 K, and the total weight gain is measured to be 11.7%. However, the weight gain of the cross-linked PSZ is limited to be 4.6%.

The results of FT-IR spectroscopic analysis are shown in Fig. 4. As-received PSZ presents absorptions at 3400 cm^{-1} (N–H), 2950–2900 cm^{-1} (C–H), 2150 cm^{-1} (Si–H), 1250 cm^{-1} (Si–CH$_3$), 1180 cm^{-1} (N–H) and 840–1020 cm^{-1} (Si–N–Si)[24,25] (Fig. 4a). After curing in air at 543 K, PSZ shows a remarkable decrease in absorption intensity at 2150 cm^{-1} (Si–H), and presents a new broad absorption band at 3480 cm^{-1} assigned to Si–OH groups (Fig. 4b).
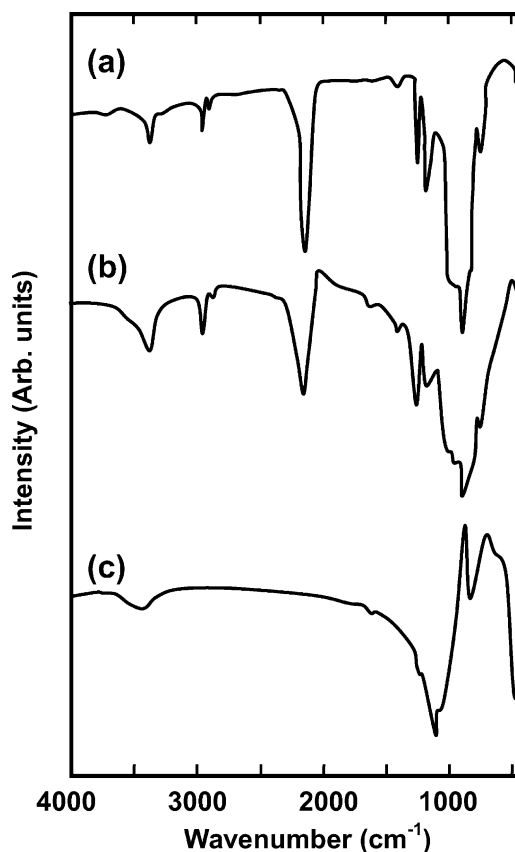

Fig. 4. FT-IR spectra of (a) as-received PSZ, (b) PSZ cured at 543 K in air, and (c) amorphous silica synthesized by cross-linking of PSZ at 543 K in N$_2$ followed by heat treatment at 873 K in air for 10 h.

FT-IR analysis was also performed on the cross-linked PSZ, and the spectrum revealed that PSZ kept the initial chemical structure. Finally, by heat treatment in air at 873 K for 10 h, the two samples of the cured and cross-linked PSZ were converted into amorphous silica, and FT-IR analysis of the 873 K heat-treated samples resulted in a detection of Si−O strong absorption band at 1120 cm^{-1}. As a typical result, the spectrum of the cross-linked PSZ-derived amorphous silica is shown in Fig. 4c.

As the Si−H absorption intensity decreased in the spectrum of the 543 K cured PSZ, the oxidation of Si−H bonds shown in Eq. (3) is confirmed as the main reaction. Then, further oxidation reactions of the cured PSZ started at 504 K. One reason for the weight loss observed at 704 to 873 K can be explained by the cleavage of Si−CH$_3$ bonds followed by the evolution of CH$_4$.[32] These oxidation reactions of the cross-linked PSZ also proceeded in air, and finally PSZ was converted into amorphous silica. However, the cross-linked PSZ initially had no stable Si−O−Si linkages, and the lower weight gain observed for this sample is thought to be due to the continuous volatilization of the lightweight molecules.

To study the effect of the difference in conversion behavior between the cured and cross-linked PSZ on the porous structure of the amorphous silica, PSZ was penetrated into a Si$_3$N$_4$ porous substrate with pore size range of 40–100 nm (shown in Fig. 1), and converted into amorphous silica by the two different heating conditions. Then, pore-size distribution analysis was performed on each sample. The results are shown in Fig. 5. The distribution curve of the cured PSZ shows a broad peak at around 0.5 nm. In addition to the micropores around 0.5 nm, the distribution curve of the cross-linked PSZ reveals the existence of a larger amount of mesopores having a size range of about 2–10 nm. It turns out from the results shown in Fig. 5, the cross-linking in N$_2$ at 543 K of the PSZ is effective for the mesoporous structure development of the PSZ-derived amorphous silica within the porous substrate, and the continuous volatilization of the light weight
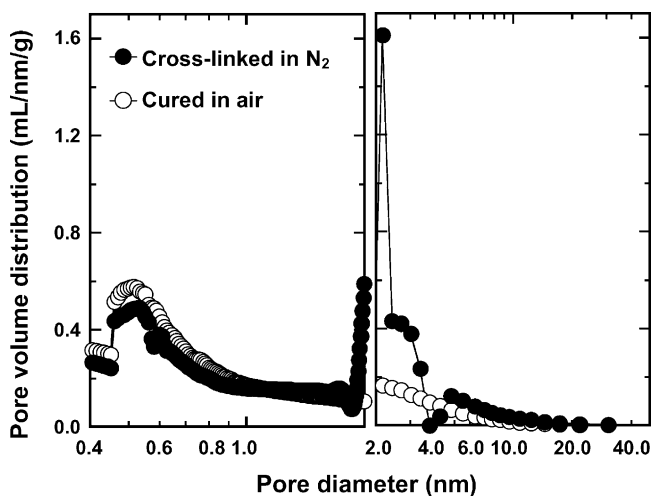
molecules in the PSZ is considered to act an important role for the formation of mesopores.

Based on the results obtained shown above, amorphous silica membrane was fabricated on a Si$_3$N$_4$ porous substrate as follows: To prepare a fine mesoporous intermediate layer, PSZ was spin-coated and penetrated into near the surface layer of the porous substrate. The surface layer was converted into mesoporous amorphous silica/Si$_3$N$_4$ composite layer by cross-linking of PSZ at 543 K in N$_2$ followed by heat treatment at 873 K in air. Then, to fabricate an active molecular sieving thin layer, a PSZ precursor film was fabricated on the surface of the mesoporous composite layer by spin-coating. The precursor film was converted into microporous amorphous silica by curing at 543 K followed by an additional heat treatment at 873 K in air.

3.2. Gas permeation properties and microstructure of amorphous silica membrane

Permeances of PSZ-derived amorphous silica membrane on a Si$_3$N$_4$ porous substrate are plotted in Fig. 6. At 423 K, the permeances of H$_2$, CO$_2$, N$_2$, CH$_4$ and CO are 3.5 × 10^{-9} mol/m^2 s Pa, 6.4 × 10^{-11} mol/m^2 s Pa, 4.2 × 10^{-11} mol/m^2 s Pa, 1.7 × 10^{-11} mol/m^2 s Pa and 8.1 × 10^{-12} mol/m^2 s Pa, respectively. The permeance of each gas increases with increasing permeation temperature, and follows the Arrhenius low.

According to mechanisms of Knudsen diffusion and viscous flow, permeation of a gas molecule in a porous medium leads to decreasing permeance with increasing temperature. The observed increasing permeance clearly indicates that the dominant mechanism of each gas permeance is the activated diffusion. The H$_2$ permselectivity increases with increasing the permeation temperature, and the permeance at 573 K

Fig. 5. Pore-size distribution of PSZ-derived amorphous silica within a Si$_3$N$_4$ porous substrate.
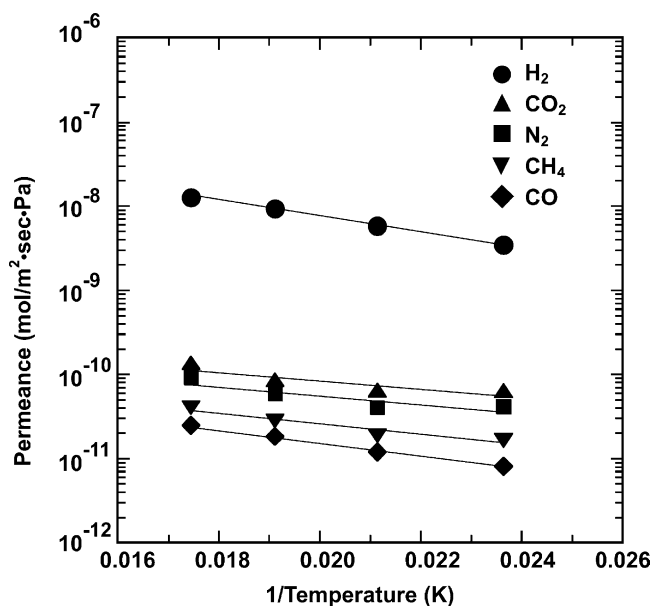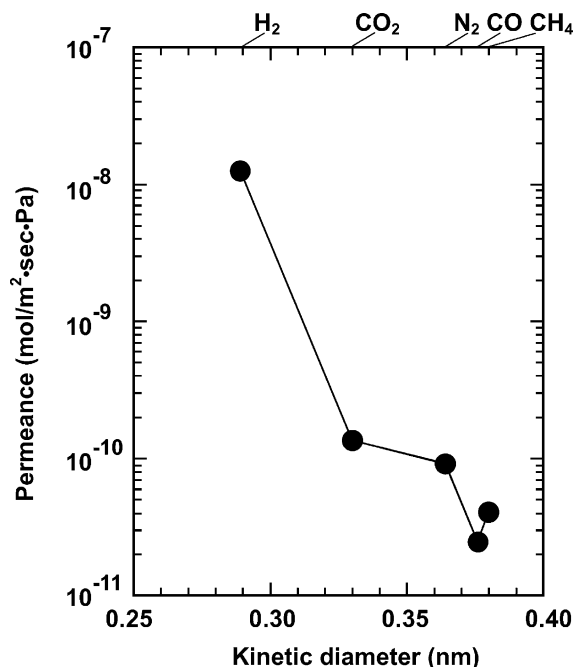

Fig. 6. Arrhenius plots of permeances of PSZ-derived amorphous silica membrane.

Fig. 7. Permeances at 573 K of PSZ-derived amorphous silica membrane vs. kinetic diameters of the permeating gas.

Fig. 8. H_2/N_2 permselectivity at 573 K of PSZ-derived amorphous silica membrane in comparison with those in literature. The literature data measured at permeation temperatures ranging from 423 to 673 K were taken for the comparison.

versus the kinetic diameter of a permeating gas molecule is plotted in Fig. 7. The molecular sieving effect is clearly observed for this membrane. The permeances of H_2, CO_2, N_2, CO and CH_4 are 1.3×10^{-8} mol/m^2 s Pa, 1.4×10^{-10} mol/m^2 s Pa, 9.2×10^{-11} mol/m^2 s Pa, 2.5×10^{-11} mol/m^2 s Pa and 4.0×10^{-11} mol/m^2 s Pa, respectively, and the permselectivities of H_2/CO_2, H_2/N_2, H_2/CO, and H_2/CH_4 are measured to be 93, 141, 520 and 325, respectively. The H_2 permselectivities are much higher than the values of 4.67 for H_2/CO_2, 3.73 for H_2/N_2 or CO, and 2.82 for H_2/CH_4, which are calculated under the assumption of Knudsen diffusion mechanism.

Generally, the permeance of a gas molecule through a microporous membrane decreases as the diameter of a gas molecule increases. However, as shown in Fig. 7, CH_4, the gas molecule with the largest kinetic diameter, has higher permeability compared with that of CO. This can be explained by the chemical nature of the PSZ-derived amorphous silica membrane itself. As mentioned above, CH_4 is thought to be one of the evaporating species during the thermal conversion of PSZ. Therefore, CH_4-selective diffusion channel sites may form which would explain the result of the permeation experiment. The CH_4 diffusion is partially enhanced by the surface diffusion mechanism. Similar explanations have been given by Kusakabe et al.,[17] and Li et al.[18] in the case of CO_2 in polycarbosilane-derived Si−C−O membranes.

Comparing with the amorphous silica membranes synthesized by CVD[9,10] or sol–gel[11,13,14,16] method and polymeric precursor-derived Si−C−O membranes[17,19] in literature, the H_2/N_2 permselectivity at 573 K of the amorphous silica membrane synthesized in this study is plotted in Fig. 8. The literature data measured at permeation temperatures ranging
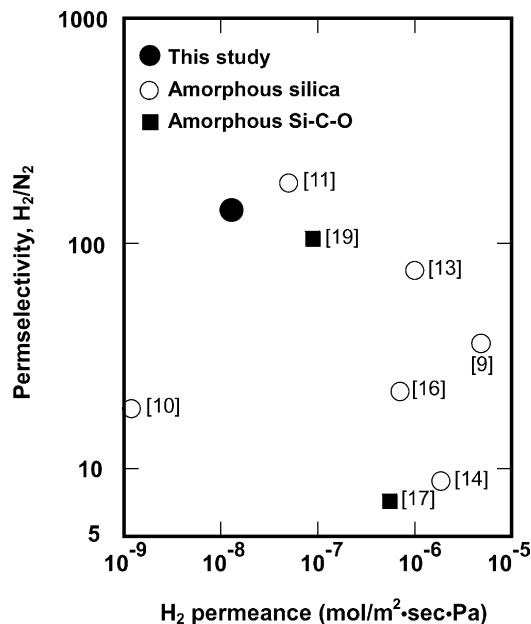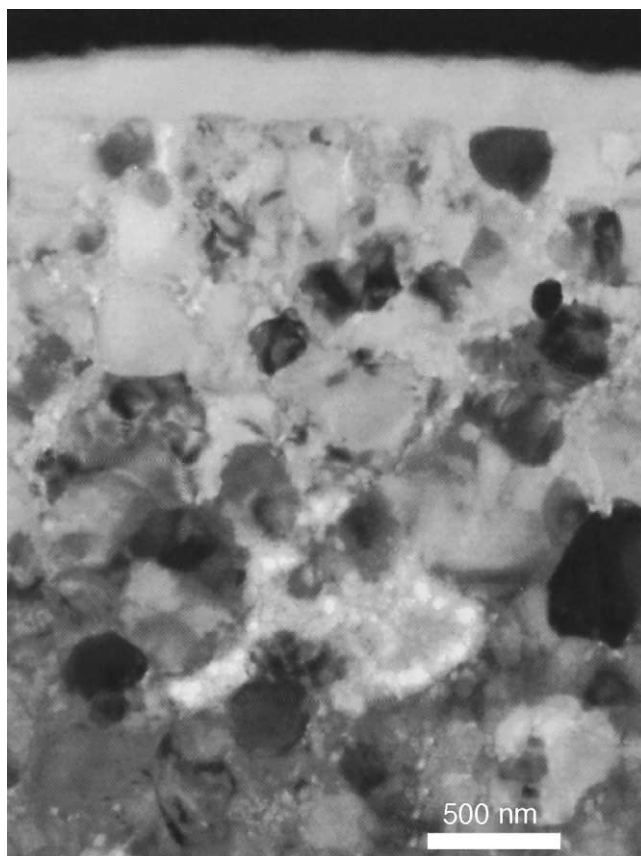

Fig. 9. Cross-sectional TEM image of PSZ-derived amorphous silica membrane fabricated on a Si_3N_4 porous substrate.
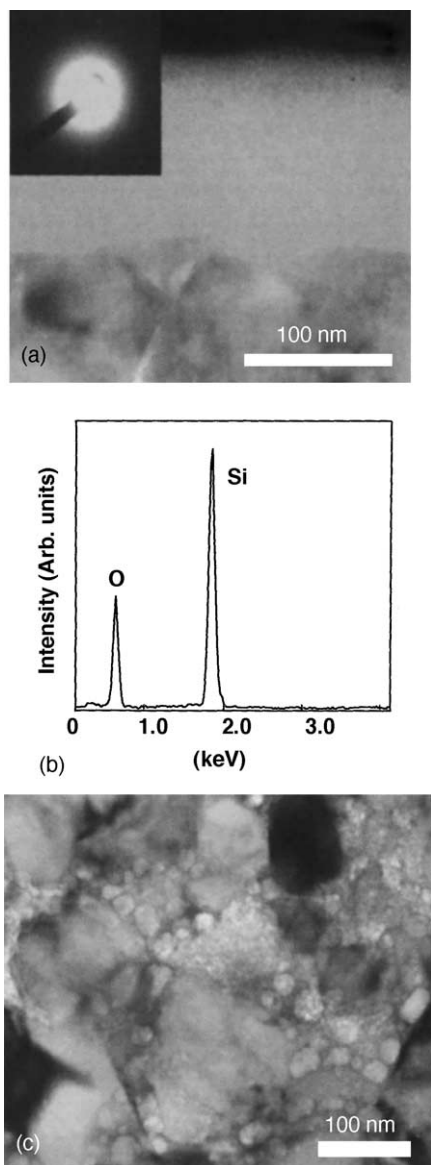
Fig. 10. TEM images showing (a) a defect-free thin layer located on the surface substrate and SADP obtained from the thin layer, (b) EDS spectra obtained from the thin layer shown in (a), and (c) PSZ-derived amorphous silica within the porous substrate.

from 423 to 673 K are taken for the comparison. Relatively high H_2/N_2 permselectivity is successfully achieved for the PSZ-derived amorphous silica membrane in this study.

A cross-sectional TEM image of the amorphous silica membrane fabricated on a Si_3N_4 porous substrate is shown in Fig. 9. A defect-free thin layer with a thickness of about 150 nm is homogeneously deposited on the surface of mesoporous amorphous silica/Si_3N_4 composite layer. The selected area electron diffraction pattern (SADP, Fig. 10a) and EDS spectra (Fig. 10b) obtained from the thin layer reveal that the PSZ has been fully converted into amorphous silica. A typical TEM image of the PSZ-derived amorphous silica/Si_3N_4 composite layer is shown in Fig. 10c. PSZ-derived amor-

phous silica is continuously located as irregular-shaped particles having a size range of about 10–100 nm.

Based on the results of the TEM microstructure characterization, PSZ-derived amorphous silica membrane is successfully fabricated on a Si_3N_4 porous substrate as designed, and the defect-free thin layer located on the substrate surface is conformed as an active molecular-sieving layer for hydrogen separation.

4. Summary

In this study, an amorphous silica membrane was fabricated by thermal conversion in air of commercially available PSZ on a Si_3N_4 porous substrate. To prepare a fine mesoporous intermediate layer for supporting an active molecular sieving thin layer, PSZ was spin-coated and penetrated into near the surface layer of the porous substrate. Then, the surface layer was converted into mesoporous amorphous silica/Si_3N_4 composite layer by cross-linking of PSZ at 543 K in N_2 followed by heat treatment at 873 K in air. A defect-free thin layer with a thickness of about 150 nm was successfully fabricated on the surface of the mesoporous composite layer by curing of PSZ at 543 K followed by heat treatment at 873 K in air. The PSZ-derived amorphous silica membrane exhibited H_2 permeance of 1.3×10^{-8} mol/m^2 s Pa at 573 K, and the permeability ratio of H_2/N_2 was measured to be 141. This H_2 permselectivity was comparable with other amorphous silica or silicon oxycarbide membranes in literature, and the polymer pyrolysis method investigated in this study was found to be useful for fabricating H_2 permselective amorphous silica membranes.

References

1. van Veen, H. M., Bracht, M., Hamoen, E. and Alderliesten, P. T., *Inorganic Membrane Science and Technology, Membrane Science and Technology Series*, *Vol 4*, ed. A. J. Burgraaf and L. Cot. Elsevier, Amsterdam, 1996 [pp. 641–676].
2. Jarosch, K. and de Lasa, H. I., *Chem. Eng. Sci.*, 1999, **54**, 1455–1460.
3. Kikuchi, E., *Catal. Today*, 2000, **56**, 97–101.
4. Prabhu, A. K. and Oyama, S. T., *J. Membr. Sci.*, 2000, **176**, 233–248.
5. Kurungot, S., Yamaguchi, T. and Nakao, S., *Catal. Lett.*, 2003, **86**, 273–278.
6. Gavalas, G. R., Megris, C. E. and Nam, S. W., *Chem. Eng. Sci.*, 1989, **44**, 1829–1835.
7. Tsapatsis, M. and Gavalas, G. R., *J. Membr. Sci.*, 1994, **87**, 281–296.

8. Yan, S., Maeda, H., Kusakabe, K., Morooka, S. and Akiyama, Y., *Ind. Eng. Chem. Res.*, 1994, **33**, 2096–2101.

9. Wu, J. C. S., Sabol, H., Smith, G. W., Flowers, D. L. and Liu, P. K. T., *J. Membr. Sci.*, 1994, **96**, 275–287.

10. Hwang, G.-J., Onuki, K., Shimizu, S. and Ohya, H., *J. Membr. Sci.*, 1999, **162**, 83–90.

11. Kitao, S., Kameda, H. and Asaeda, M., *Membrane*, 1990, **15**(4), 222–227.

12. Nair, B. N., Yamaguchi, T., Okubo, T., Suematsu, H., Keizer, K. and Nakao, S., *J. Membr. Sci.*, 1997, **135**, 237–243.

13. de Vos, R. M. and Verweij, H., *J. Membr. Sci.*, 1998, **143**, 37–51.

14. de Vos, R. M., Maier, W. F. and Verweij, H., *J. Membr. Sci.*, 1999, **158**, 277–288.

15. Yoshida, K., Hirano, Y., Fujii, H., Tsuru, T. and Asaeda, *J. Chem. Eng. Jpn.*, 2001, **34**, 523–530.

16. Kusakabe, K., Shibao, F., Zhao, G., Sotowa, K.-I., Watanabe, K. and Saito, T., *J. Membr. Sci.*, 2003, **215**, 321–326.

17. Kusakabe, K., Ii, Z. Y., Maeda, H. and Morooka, S., *J. Membr. Sci.*, 1995, **103**, 175–180.

18. Li, Z. Y., Kusakabe, K. and Morooka, S., *J. Membr. Sci.*, 1996, **118**, 159–168.

19. Lee, L. L. and Tsai, D.-S., *J. Am. Ceram. Soc.*, 1999, **82**, 2796–2800.

20. CLARIANT (JAPAN) K.K. Technical information, "ALCEDAR COAT®", 25 July 2000.

21. Iwamoto, Y., Volger, W., Kroke, E., Saitou, T., Matsunaga, K. and Riedel, R., *J. Am. Ceram. Soc.*, 2002, **84**, 2170–2178.

22. Saito, A. and Foley, H. C., *AIChE J.*, 1991, **37**, 429–436; Saito, A. and Foley, H. C., *Microporous Mater.*, 1995, **3**, 531–542.

23. Barrett, P., Joyner, L. G. and Halenda, P. H., *J. Am. Chem. Soc.*, 1951, **73**, 373–380.

24. Kato, K., Sasaki, Y., Osada, K., Hirayama, T. and Saka, H., *Surf. Interface Anal.*, 2001, **31**, 409–414.

25. Iwamoto, Y., Kikuta, K. and Hirano, S., *J. Mater. Res.*, 1998, **13**, 353–361.

26. Iwamoto, Y., Kikuta, K. and Hirano, S., *J. Mater. Res.*, 1999, **14**, 1886–1895.

27. Funayama, O., Tashiro, Y., Kamo, A., Okamura, M. and Isoda, T., *J. Mater. Sci.*, 1994, **29**, 4883–4888.

28. Song, Y. C., Zhao, Y., Feng, C. X. and Lu, Y., *J. Mater. Sci.*, 1994, **29**, 5745–5756.

29. Yang, D.-L., Tsai, D.-S. and Liu, H.-C., *J. Mater. Sci.*, 1995, **30**, 4463–4468.

30. Hasegawa, Y., *J. Mater. Sci.*, 1989, **24**, 1177–1190.

31. Mocaer, D., Pailler, R., Naslain, R., Richard, C., Pillot, J. P., Donogues, J. *et al.*, *J. Mater. Sci.*, 1993, **28**, 2615–2631.

32. Sugimoto, M., Shimoo, T., Okamura, K. and Seguchi, T., *J. Am. Ceram. Soc.*, 1995, **78**, 1849–1852.